Microscopic dynamics and structure of liquid ^{7}Li

1994 J. Phys.: Condens. Matter 6 8391

(http://iopscience.iop.org/0953-8984/6/41/005)

J. Phys.: Condens. Matter 6 (1994) 8391–8413. Printed in the UK

Microscopic dynamics and structure of liquid ^{7}Li

P H K de Jong, P Verkerk and L A de Graaf
Interfaculty Reactor Institute, Delft University of Technology, 2629 JB Delft, The Netherlands

Received 28 February 1994, in final form 20 June 1994

Abstract. We report an inelastic neutron scattering (INS) experiment on liquid ^{7}Li at 470 K, 526 K and 574 K using thermal neutrons. Fully corrected structure factors $S(\kappa, \omega)$ were obtained. We have assessed the quality of the data by means of the first frequency moment of $S(\kappa, \omega)$ and by the detailed balance condition. The coherent dynamic structure factor $S_c(\kappa, \omega)$ and the incoherent dynamic structure factor $S_s(\kappa, \omega)$ were separated by fitting models. We compare the data for $S_s(\kappa, \omega)$ at small κ with several models using no adjustable parameters. The Lovesey model for $S_s(\kappa, \omega)$ gives very good agreement with the experimental data at all three temperatures. $S_s(\kappa, \omega)$ is not well described by the predictions from simple diffusion, mode-coupling theory or the model of Nelkin–Ghatak. The Lovesey model also gives the best agreement with the data when we fit one parameter.

1. Introduction

In this paper we present our results of an INS experiment on liquid ^{7}Li with thermal neutrons at three temperatures (470 K, 526 K and 574 K) near the melting point. The dynamic structure factor $S(\kappa, \omega)$ of liquid ^{7}Li is a weighted sum of the coherent dynamic structure factor $S_c(\kappa, \omega)$ and the incoherent dynamic structure factor $S_s(\kappa, \omega)$ because the scattering cross sections are almost equal. In particular, $S_s(\kappa, \omega)$ is very interesting because $S_s(\kappa, \omega)$ can only be measured using neutrons and it has so far only been determined for a small number of monatomic liquids (i.e. Na [1], Ar [2]).

The dynamics of liquid lithium has been studied by inelastic x-ray scattering (IXS) experiments [3], by computer molecular dynamics (CMD) simulations [4–6], and by inelastic neutron scattering (INS) experiments [7–10]. The sound dispersion in liquid lithium, determined by IXS experiments [3] and by INS experiments with epithermal neutrons [9], is similar to other monatomic systems. The position of the sound modes follows the predictions from hydrodynamics up to $\kappa_0/2$, where κ_0 is the position of the main peak of the static structure factor $S(\kappa)$, and shifts to smaller ω for κ beyond $\kappa_0/2$. It follows from the INS experiment with epithermal neutrons [9] that the dynamics of liquid lithium at very large momentum transfers does not deviate from the free-gas behaviour. Sedlmeir [10] performed INS experiments with polarization analysis (PA) on liquid ^{7}Li at 600 K. This method has the advantage that $S_c(\kappa, \omega)$ and $S_s(\kappa, \omega)$ can be separated experimentally. A comparison of their data and the present data at 574 K shows that the data differ considerably [11]. The origin is unknown. Part of the present work has been published elsewhere [7, 8].

Deviations occur between $S(\kappa)$ of liquid lithium determined using x-rays and neutrons. It is at present unclear whether these differences are caused by improper corrections (i.e. form factor [12] or inelastic scattering [13, 14]) or if this reflects the effect of delocalized electrons. The integration of $S_c(\kappa, \omega)$ is a way to avoid the correction for inelasticity, which can be rather large for lithium due to its small mass. Comparing the $S(\kappa)$ measured

0953-8984/94/418391+23$19.50

with neutrons and x-rays might give insight in the correlations between electrons and ions (e.g. liquid Li [15] or liquid Se [16]). $S(\kappa)$ at small κ for liquid metals is sensitive for testing potentials but is often very difficult to measure. The dynamics is probably a property sensitive to the potential over a larger κ range. By measuring $S(\kappa, \omega)$ we can provide data to test potentials for liquid lithium.

The aims of our investigation are therefore threefold: to study the dynamics in liquid ^{7}Li near the melting point as a function of temperature and compare the results with predictions from theory, to compare $S(\kappa)$ determined by integration over $S_c(\kappa, \omega)$ with $S(\kappa)$ from literature, and finally, to provide data to test potentials for liquid lithium.

We describe the theory in section 2, the experiment in section 3, and the results in section 4. The discussion of the results and the conclusions are given in sections 5 and 6, respectively.

2. Theory

In this section we briefly describe the models for $S_s(\kappa, \omega)$ and $S_c(\kappa, \omega)$ that we use in this paper. The reader is referred to the original papers for full details.

In the hydrodynamic limit the single-particle dynamics is described by simple diffusion:

$$S_s^{SD}(\kappa, \omega) = \frac{1}{\pi} \frac{\mathcal{D}\kappa^2}{\omega^2 + (\mathcal{D}\kappa^2)^2}$$

where $\mathcal{D}$ is the self-diffusion coefficient.

The mode-coupling theory of de Schepper and Ernst [17], which describes the coupling between diffusive and transversal modes, gives the first-order correction for $S_s(\kappa, \omega)$:

$$S_s^{MC}(\kappa, \omega) = S_s^{SD}(\kappa, \omega) + \frac{1}{\pi} \frac{1}{\mathcal{D}\kappa\kappa^*} \mathrm{Re}\, G\left(\frac{i\omega + \mathcal{D}\kappa^2}{\delta \mathcal{D}\kappa^2}\right) + O\left[\sqrt{\kappa}\, f(\omega/\kappa^2)\right] \tag{2.1}$$

where

$$\kappa^* = 16\pi\beta M n_s \mathcal{D}^2 \qquad \beta = 1/k_B T$$

with k_B the Boltzmann constant and T the temperature, M the atomic mass, $\delta = \mathcal{D}/(\mathcal{D} + \nu)$ and ν is the kinematic viscosity. The function G is given by

$$G(z) = \tan^{-1}\left(\frac{1}{\sqrt{z-1}}\right) - \frac{(z-2)\sqrt{z-1}}{z^2}.$$

The Lovesey model [18] for $S_s(\kappa, \omega)$ is given by

$$S_s^{LO}(\kappa, \omega) = \frac{1}{\pi} \frac{\tau_\kappa \delta_1 \delta_2}{\omega^2 \tau_\kappa^2 (\omega^2 - \delta_1 - \delta_2)^2 + (\omega^2 - \delta_1)^2} \tag{2.2}$$

where

$$\delta_1 = \kappa^2/\beta M \qquad \delta_2 = 2\delta_1 + \Omega^2.$$

Here Ω is an integral over the radial pair distribution function and the second derivative of the pair potential (see equation (3.2) in [18]); τ_κ is the integral over the third-order memory function. By postulating $S_s^{LO}(\kappa, \omega = 0) = S_s^{SD}(\kappa, \omega = 0)$ one obtains

$$\tau_\kappa^{-1} = \beta M \mathcal{D} \delta_2.$$

The model of Nelkin–Ghatak for $S_s(\kappa, \omega)$ [19] is

$$S_s^{NG}(\kappa, \omega) = \frac{1}{\pi\alpha} \frac{U(1-U) - V^2}{(1-U)^2 + V^2} \tag{2.3}$$

where $U(x, y) = yu(x, y)\sqrt{\pi}$, $V(x, y) = yv(x, y)\sqrt{\pi}$ and

$$W(x + iy) = u(x, y) + iv(x, y)$$

is the probability function for complex arguments. The reduced variables x and y are defined by

$$x = -\frac{\omega}{\kappa v_0\sqrt{2}} \qquad y = \frac{\alpha}{\kappa v_0\sqrt{2}}$$

where $v_0^2 = k_B T/M$ and α denotes the average collision frequency. This model has the correct large-κ limit of $S_s(\kappa, \omega)$. It also has the correct small-κ limit provided we set $\alpha = v_0^2/\mathcal{D}$.

According to kinetic theory the coherent dynamic structure factor $S_c(\kappa, \omega)$ can be decomposed into an infinite set of Lorentzians [20, 21]. The first three extended hydrodynamics modes dominate for $\kappa \leqslant l^{-1}$, where l is the mean free path between collisions

$$S_c^{EH}(\kappa\,\omega) = S(\kappa)\,\mathrm{Re}\sum_{j=-1}^{+1} \frac{1}{\pi} \frac{A_j(\kappa)}{i\omega + z_j(\kappa)} \tag{2.4}$$

where $A_0(\kappa)$ and $z_0(\kappa)$ are real, and $A_{\pm1}(\kappa)$ and $z_{\pm1}(\kappa)$ are either real or complex conjugate pairs. This model passes in the small-κ limit into the Landau–Placzek triplet, which consists of two Brillouin lines ($j = \pm1$) located at $\omega_s \approx \pm \mathrm{Im}\, z_{\pm1}(\kappa) = c_s\kappa$, with c_s the sound velocity and one Rayleigh line ($j = 0$). The thermal diffusion coefficient a_{ion} is given by z_0/κ^2, the sound attenuation coefficient by $\mathrm{Re}\, z_{\pm1}(\kappa)/\kappa^2$.

The Enskog mean free path l_E is $(n_s\pi\sigma^2 g(\sigma)\sqrt{2})^{-1}$, where σ is the hard-sphere diameter and $g(\sigma)$ is the pair correlation function $g(r)$ for hard-spheres at $r = \sigma$. We determined σ from a fit of the main peak of the hard-sphere $S(\kappa)$ to the main peak of the experimental $S(\kappa)$. For the determination of σ we use neutron data at 470 K and 595 K [14] and x-ray data at 523 K [22]. For lithium at 470 K, 523 K and 595 K we find 0.272 nm, 0.271 nm and 0.269 nm, respectively. The corresponding l_E in liquid ^{7}Li is about 0.014 nm. Hence the three extended hydrodynamic modes dominate for κ up to $\simeq 70\,\mathrm{nm}^{-1}$.

3. Experiment

We have performed the experiment with the time-of-flight (TOF) spectrometer RKS at the 2 MW reactor of our institute. We used an incident energy (wavelength) of 20.5 meV

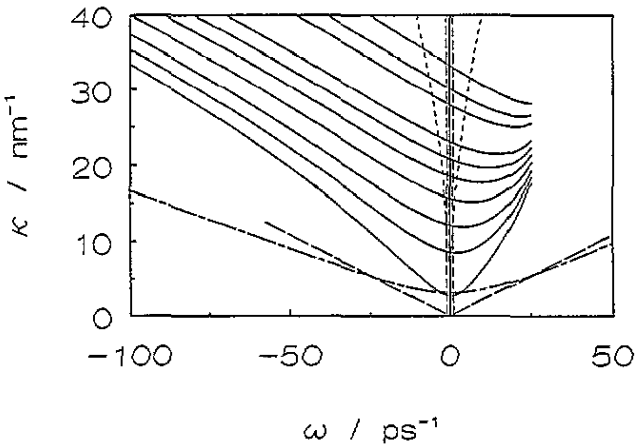

Figure 1. Kinematically accessible κ–ω plane at $E_0 = 20.5$ meV. The curves drawn indicate detectors at scattering angles of 4.96°, 15.7°, 22.2°, 28.8°, 34.2°, 38.6°, 43.0°, 52.8°, 57.2° and 63.8°, respectively. Broken vertical line: half width at half maximum (HWHM) of the resolution, short broken line: HWHM of $S_s(\kappa, \omega)$ at 470 K according to hydrodynamics, broken line: expected position of the collective modes up to $\frac{1}{2}\kappa_0$. The long broken line denotes the integration path through κ–ω space for a detector with a scattering of 2° at an incident wavelength of 0.0695 nm.

Table 1. Cross sections for ^{6}Li, ^{7}Li, our ^{7}Li specimen (from [45]) and vanadium [46]. The bound atom cross sections for coherent and incoherent scattering are denoted by σ_c and σ_i, respectively. The absorption cross section is denoted by σ_a.

Cross section (b)	^{6}Li	^{7}Li	^{7}Li (99.975 at.%)	V
σ_c	0.51(5)	0.619(6)	0.619(6)	0.02
σ_i	0.46(2)	0.68(3)	0.68(3)	4.96
$\sigma_s = \sigma_c + \sigma_i$	0.97(5)	1.30(3)	1.30(3)	4.98
σ_a (0.18 nm)	940(4)	0.0454(3)	0.280(1)	5.08

($\lambda_0 = 0.200$ nm). The half width at half maximum of the energy resolution varies from 0.69 meV at the smallest scattering angle (4.96°) to 0.8 meV at the largest scattering angle (63.8°). In total 52 detectors were used. The beam size is $2.5 \times 10\,\text{cm}^2$. The flux at the sample position is $800\,\text{n cm}^{-2}\,\text{s}^{-1}$. The kinematically accessible κ–ω plane is given in figure 1.

We performed measurements on lithium enriched in ^{7}Li because ^{6}Li strongly absorbs neutrons (table 1). The lithium sample is contained in a niobium cell (see figure 2) specially designed for a vertical scattering geometry such as the RKS. The cell can be used from the melting point (454 K) to about 1200 K. The sample cell was filled in the helium-filled glovebox of the Laboratory of Solid State Physics at the University of Groningen to avoid the reactions of lithium with oxygen and nitrogen. The cell was transported under argon gas to the electron beam welding facility [23], where it was sealed under vacuum.

The sample cell was heated by means of two separate heating elements which were connected to the ends of the cell. The temperature of the cell was measured by two chromel–alumel thermocouples positioned in the ends of the cell. The calculated temperature gradient over the sample cell in the present temperature range was about 3 K and the stability in time was about 1 K. An aluminium foil (of 0.1 mm thickness) was used as a thermal radiation shield. The cell and elements were placed in an aluminium vacuum containment during the

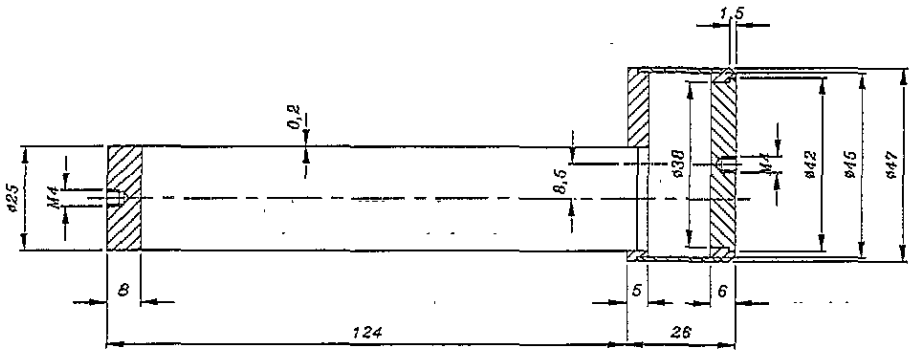

Figure 2. Drawing of the niobium sample cell. Dimensions in mm.

experiment.

Apart from the measurements on ^{7}Li at 470 K, 526 K and 574 K (each for about 90 h), the scattering from an identical niobium cell (for 112 h), a vanadium spiral foil in an aluminium cell (for 160 h) and the empty aluminium cell (for 164 h) were also measured. The niobium cell was filled with ^{3}He gas (about 450 mbar) in order to get the same transmission (88%) as the cell filled with ^{7}Li. The transmission of the sample cell is not strongly temperature dependent because the densities at these three temperatures (see table 2) are almost the same.

Table 2. Some properties of liquid Li and liquid ^{7}Li. The properties followed by an asterisk refer to ^{7}Li. The data were taken from [29, 46–48]. c_p (c_V) is the specific heat at constant pressure (volume) and $S(0)$ is the long-wavelength limit of $S(\kappa)$. The kinematic viscosity and self-diffusion coefficient are given in nm^2ps^{-1} and 10^{-3} nm^2ps^{-1}, respectively. The value of the average collision frequency in the hydrodynamic limit $\alpha(0)$ is calculated using the tracer data from Löwenberg and Lodding [29] for $\mathcal{D}$. Ω denotes the Einstein frequency. Ω at 526 K and at 574 K were calculated from the theoretical result at 470 K of González [32] using the suggested relation of Levesque and Verlet [33].

Property	Value		
Melting point T_m	453.7 K		
Atomic weight ^{7}Li $M*$	7.016 g mol^{-1}		
	$T = 470$ K	$T = 526$ K	$T = 574$ K
Number density n_s (nm^{-3})	44.5	44.1	43.8
$\gamma = c_p/c_V$	1.07	1.08	1.09
Kin. viscosity $\nu*$	1.10(1)	0.965(8)	0.881(8)
Self-diffusion $\mathcal{D}*$ NMR [30]	6.35(50)	8.40(55)	10.1(6)
Self-diffusion $\mathcal{D}*$ tracer [29]	6.5(2)	9.0(5)	11.2(2)
$S(0)$	0.027	0.033	0.037
$\Omega*$ (ps^{-1})	41.0	41.8	42.4
$\alpha(0)*$ (ps^{-1})	85.7	69.2	60.7
Sound velocity c_s (m s^{-1})	4554	4510	4481

The data were corrected for background, detector efficiency, multiple scattering, self-shielding and TOF resolution, normalized absolutely using the vanadium measurement and interpolated to a rectangular κ–ω grid using the methods given in [24]. A few typical TOF

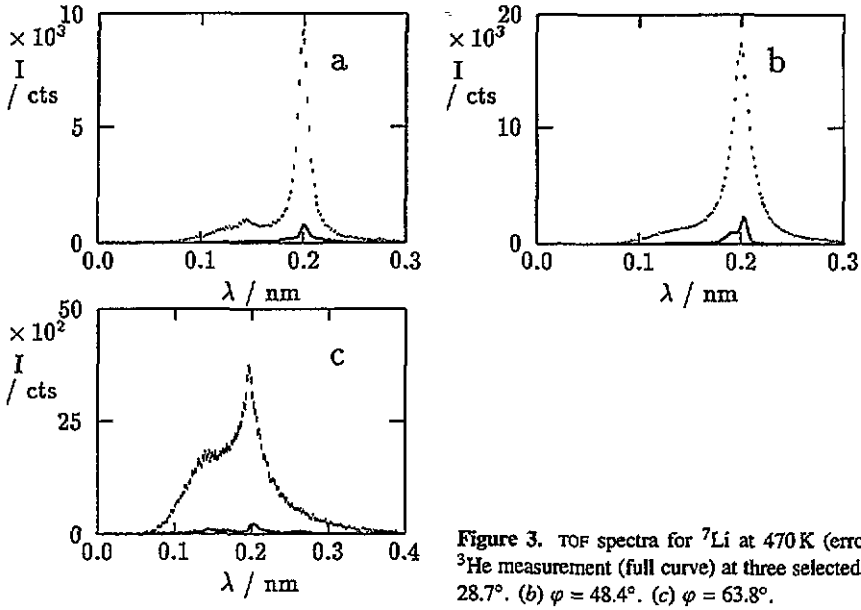

Figure 3. TOF spectra for ^{7}Li at 470 K (error bars) and the ^{3}He measurement (full curve) at three selected angles. (*a*) φ = 28.7°. (*b*) φ = 48.4°. (*c*) φ = 63.8°.

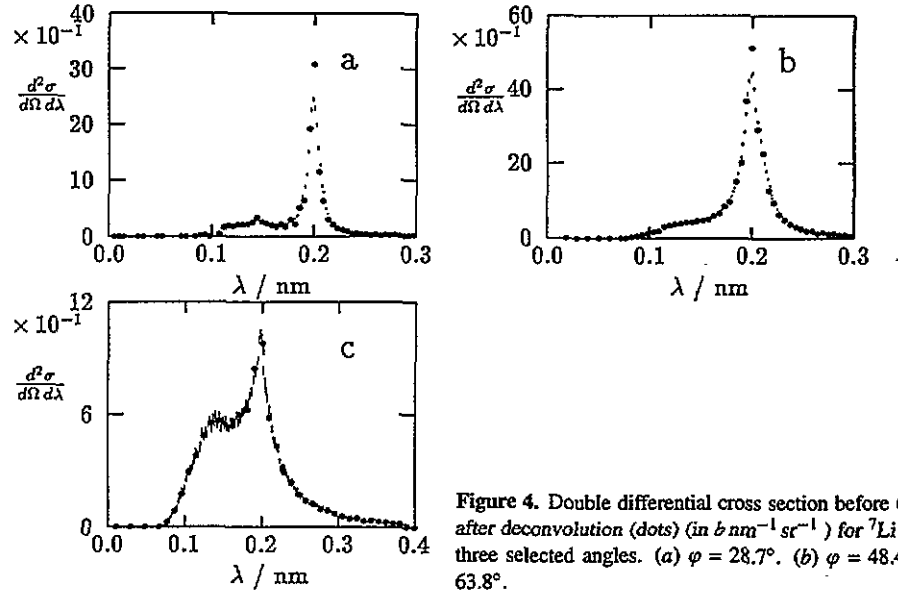

Figure 4. Double differential cross section before (errors) and after deconvolution (dots) (in $b\,nm^{-1}\,sr^{-1}$) for ^{7}Li at 470 K at three selected angles. (*a*) φ = 28.7°. (*b*) φ = 48.4°. (*c*) φ = 63.8°.

spectra for liquid ^{7}Li and the ^{3}He measurement are given in figure 3. The subtraction of the background scattering from the ^{7}Li spectra is straightforward because we performed a ^{3}He measurement.

The resolution correction is unsatisfactory at small angles. Consequently, the smallest scattering angle providing useful data is 20.1° ($\kappa_{el} = 4\pi \sin(\varphi/2)/\lambda_0 = 11.0\,nm^{-1}$) for 470 K, 19.0° ($\kappa_{el} = 10.4\,nm^{-1}$) for 526 K and 15.7° ($\kappa_{el} = 8.5\,nm^{-1}$) for 574 K. In figure 4 we show a few spectra before and after the resolution correction. The spectra at large angles are not strongly affected by the resolution.

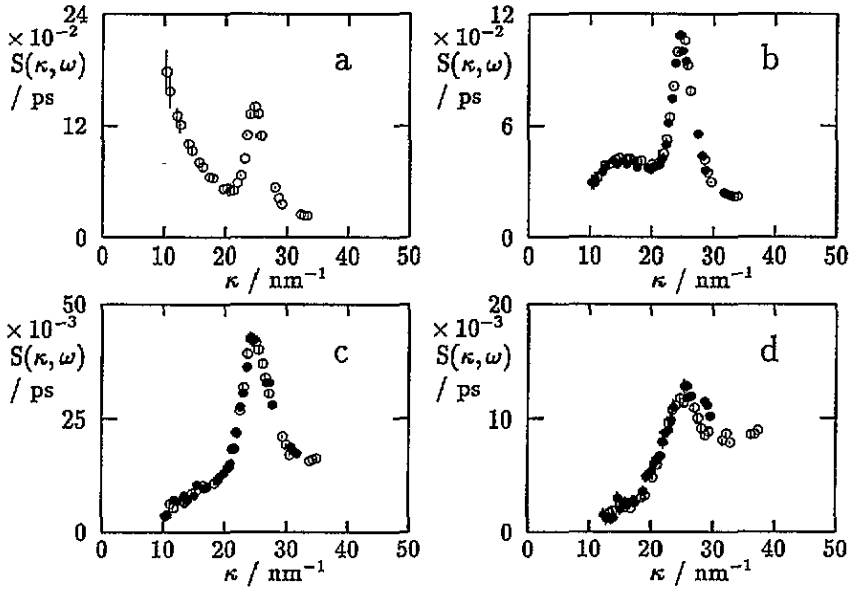

Figure 5. $S(\kappa, \omega)$ for ^{7}Li at 526 K. Circles: energy-gain data; dots: energy-loss data. (*a*) $\omega = 0$ ps^{-1}. (*b*) $|\omega| = 2$ ps^{-1}(*c*) $|\omega| = 6$ ps^{-1}. (*d*) $|\omega| = 15$ ps^{-1}.

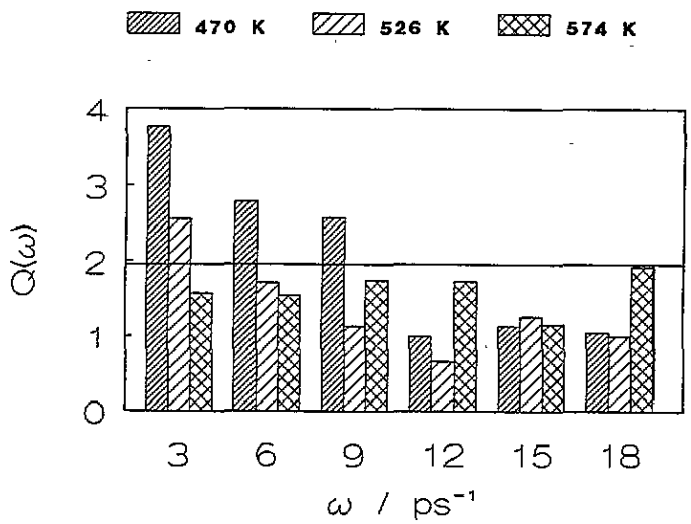

Figure 6. Quality factors Q for ^{7}Li at 470 K, 526 K and 574 K. Full line: 95 % confidence limit.

$S(\kappa, \omega)$ is related to the double-differential cross section $d^2\sigma/d\Omega d\lambda$ by

$$S(\kappa, \omega) = \frac{m}{\sigma_s \pi \hbar} \frac{\lambda^4}{\lambda_0} \frac{d^2\sigma}{d\Omega d\lambda} \tag{3.1}$$

where m is the neutron mass, $\hbar$ is the Planck constant divided by 2π, σ_s denotes the bound

atom scattering cross section and λ denotes the wavelength of the scattered neutron. We have converted our data to classical $S(\kappa, \omega)$ using the approximation of Aamodt and co-workers [25] to allow for a comparison with classical models for $S(\kappa, \omega)$. In figure 5 we show the fully corrected $S(\kappa, \omega)$ of liquid ^{7}Li at 526 K at constant ω. The energy-gain data are in good agreement with the energy-loss data. We have calculated the quality factor Q (defined in (22) in [24]) in order to assess the quality of the data in a quantitative manner. The Q values (see figure 6) are in reasonable agreement with the expectation value of Q (1). The deviations at smaller ω and lower temperature reflect the resolution effect. In figure 7 we show a few typical $S(\kappa, \omega)$ at constant κ for the three temperatures. The frequency moments $\langle \omega^n \rangle$ of the dynamic structure factor $S(\kappa, \omega)$ defined by

$$\langle \omega^n \rangle = \int_{-\infty}^{\infty} \mathrm{d}\omega \, \omega^n S(\kappa, \omega) \tag{3.2}$$

can also be used to assess the quality of the data. The theoretical values for $n = 0$ and $n = 1$ are

$$\langle \omega^0 \rangle = \frac{\sigma_c}{\sigma_s} S(\kappa) + \frac{\sigma_i}{\sigma_s} \tag{3.3}$$

$$\langle \omega^1 \rangle = \omega_R = \frac{\hbar \kappa^2}{2M} \tag{3.4}$$

where σ_c and σ_i denote the coherent and incoherent scattering cross sections (table 1) and $\hbar\omega_R$ is the recoil energy. In general, the integral in (3.2) cannot be calculated exactly using experimental data because of the limited ω range. Nevertheless, for $\kappa \geqslant 22\,\mathrm{nm}^{-1}$, where the experimental accessible ω range allows for the calculation of the integral in (3.2), we find good agreement between the experimental $\langle \omega^1 \rangle$ and the theoretical value (see figure 8). For κ smaller than $22\,\mathrm{nm}^{-1}$ too much of $S(\kappa, \omega)$ extends beyond the maximum ω and numerical integration is not possible.

An assessment of the quality of the data by using $\langle \omega^0 \rangle$ is not useful. Firstly, $\langle \omega^0 \rangle$ at small κ consists of $S_s(\kappa, \omega)$ and a part of $S_c(\kappa, \omega)$ because experiments [3, 9] show that a large fraction of $S_c(\kappa, \omega)$ falls beyond the maximum accessible ω in the present experiment. Secondly, deviations occur between the $S(\kappa)$ data from literature near κ_0 for temperatures close to 470 K. We will compare the present $S(\kappa)$ and $S(\kappa)$ from literature in section 4.

4. Results

4.1. Static structure factor

We extract $S(\kappa)$ from $\langle \omega^0 \rangle$ using (3.3) and the cross sections from table 1. In figure 9 we show the present $S(\kappa)$ and $S(\kappa)$ from literature (listed in [26]). The present $S(\kappa)$ at 470 K is for $\kappa \leqslant 23\,\mathrm{nm}^{-1}$, in agreement with x-ray data at 463 K [22] and 464 K [13], and with neutron data at 470 K [14]. The height of the main peak of the present $S(\kappa)$ is furthermore in agreement with the neutron data at 470 K. The present $S(\kappa)$ at 470 K deviates from the three $S(\kappa)$ from literature for κ beyond $26\,\mathrm{nm}^{-1}$; $S(\kappa)$ at 526 K is in good agreement with x-ray data at 523 K [22] and $S(\kappa)$ at 574 K is in good agreement with neutron data at 595 K [14].

4.2. Separation of the coherent and incoherent contributions

At small κ, $S(\kappa, \omega)$ of liquid ^{7}Li consists of predominantly $S_s(\kappa, \omega)$ due to the low value of $S(0)$ (see table 2), the limited ω range of the spectrometer and the large sound velocity (see figure 1). The widths of these contributions differ by about a factor ten (see next subsection): $S_c(\kappa, \omega)$ is much broader than $S_s(\kappa, \omega)$. This enables us to determine $S_s(\kappa, \omega)$ at small κ by correcting for $S_c(\kappa, \omega)$. The areas and the widths of $S_s(\kappa, \omega)$ and $S_c(\kappa, \omega)$ become comparable in the κ region where $S(\kappa)$ has its main peak. Consequently, we distinguish two regimes: a κ regime where $S_s(\kappa, \omega)$ dominates $S(\kappa, \omega)$ and a κ regime where $S(\kappa)$ has its main peak.

4.2.1. Dynamics at small κ. In the hydrodynamic limit $S_s(\kappa, \omega)$ becomes a Lorentzian and $S_c^{EH}(\kappa, \omega)$ predicts a central Lorentzian and two shifted Lorentzians located at $c_s\kappa$ which fall beyond the accessible ω range (see table 2 and figure 1). We have fitted our data for each κ separately with a sum of two Lorentzians in order to determine the incoherent contribution. We use one Lorentzian for $S_s(\kappa, \omega)$ and one Lorentzian for the central line of $S_c(\kappa, \omega)$. The number of free parameters is reduced to three by fixing the area of one of the Lorentzians to σ_i/σ_s (0.523), the expected area of $S_s(\kappa, \omega)$. The root mean square deviation (RMSD) averaged over the κ values is 1.4 for 470 K, 0.9 for 526 K and 1.0 for 574 K. The RMSD is defined by

$$\text{RMSD} = \left((N-p)^{-1} \sum_{i=1}^{N} \frac{\Delta_i^2}{\text{var}_i} \right)^{1/2} \tag{4.1}$$

where N denotes the number of data points, p denotes the number of parameters, Δ_i is the difference between the experimental data and the model, and var_i is the estimated variance of the experimental data.

The experimental incoherent dynamic structure factor $S_s'(\kappa, \omega)$ is obtained by subtracting the Lorentzian with the variable area from the experimental $S(\kappa, \omega)$. The correction for coherent scattering is typically of the order of 1–2% for $S_s'(\kappa, \omega = 0)$.

Firstly, we will investigate the agreement between the experimental data and the four models for $S_s(\kappa, \omega)$, namely $S_s^{SD}(\kappa, \omega)$, $S_s^{MC}(\kappa, \omega)$, $S_s^{LO}(\kappa, \omega)$ and $S_s^{NG}(\kappa, \omega)$, using no adjustable parameters. We study the RMSD of the model with $S_s'(\kappa, \omega)$, the reduced half width z_t/κ^2 of $S_s'(\kappa, \omega)$ and the reduced top value $\kappa^2 S_s'(\kappa, \omega = 0)$. Secondly, we will fit the models to $S_s'(\kappa, \omega)$ using one adjustable parameter.

We compare our data on ^{7}Li near the melting point with the predictions of the mode-coupling (MC) theory of de Schepper and Ernst [17] because Montfrooy and co-workers [27] found that this MC theory might well be relevant for liquid Na near the melting point. It is not to be expected that this MC theory, which describes the coupling between diffusive and transversal modes, gives a good description of the data, since the velocity autocorrelation function of liquid lithium near the melting point (computer molecular dynamics results of Canales and co-workers [28]) has a prominent negative dip.

The input parameter for $S_s^{SD}(\kappa, \omega)$ and $S_s^{MC}(\kappa, \omega)$ is $\mathcal{D}$. The input parameters for $S_s^{LO}(\kappa, \omega)$ are $\mathcal{D}$ and Ω. The input parameter α for $S_s^{NG}(\kappa, \omega)$ is determined by setting $\alpha = v_0^2/\mathcal{D}$; $\mathcal{D}$ and v have been determined experimentally for liquid ^{7}Li (see table 2). We have interpolated and extrapolated the available data to the present temperatures by making use of the models proposed by the authors. Löwenberg and Lodding [29] measured $\mathcal{D}$ of ^{7}Li using a tracer technique. Murday and Cotts [30] measured $\mathcal{D}$ of liquid ^{7}Li, liquid Na and liquid H_2O using NMR. They find that their data for liquid Na and liquid H_2O are

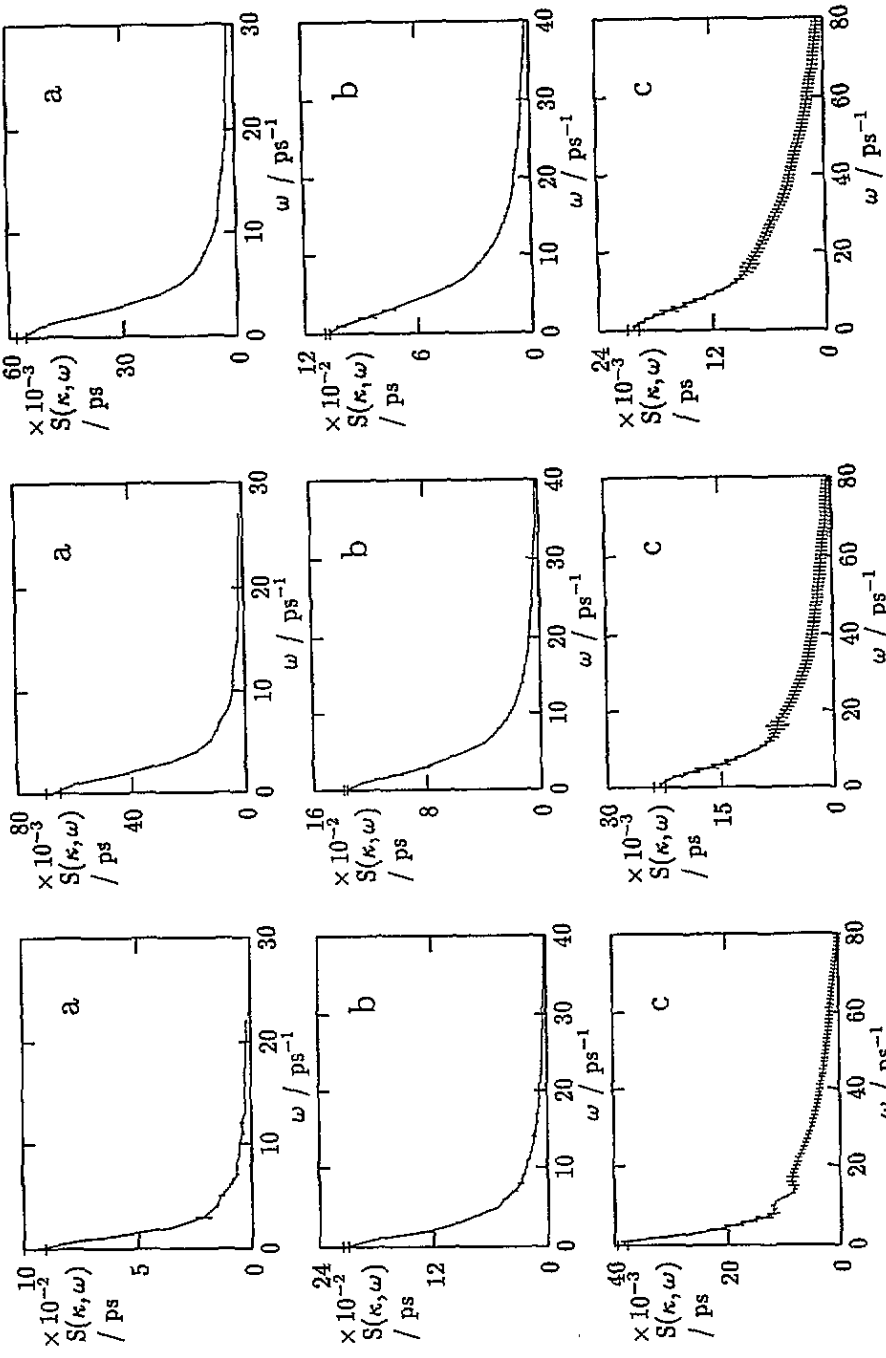

Figure 7. $S(\kappa, \omega)$ for ^{7}Li at 470 K (left), 526 K (middle) and 574 K (right) at three selected κ values. (*a*) κ = 17 nm^{-1}, (*b*) κ = 25 nm^{-1}, (*c*) κ = 33 nm^{-1}. The full curves connect the data points.

about 5% too low with respect to other published data. In the remainder of this paper we used the tracer data from Löwenberg and Lodding [29] for $\mathcal{D}$. The term Ω is an integral over the second derivative of the interatomic potential and the pair correlation function (see equation (2.37) in [31]). Gonzalez and co-workers [32] performed this integral for liquid ^{7}Li at 470 K. Their theoretical result for Ω is 41 ps^{-1}. Levesque and Verlet [33] suggest that Ω^2 varies with temperature and density as $T^{1/2}n_s^2$. We used this relation to calculate Ω at 526 K (41.8 ps^{-1}) and at 574 K (42.4 ps^{-1}).

The smallest scattering angle providing useful data and the method of separating the two contributions limit the available κ range to 14–18 nm^{-1} for 470 K, 12–18 nm^{-1} for 526 K and 11–18 nm^{-1} for 574 K. We only take into account data where $S_s'(\kappa,\omega)$ is more than 1% of the maximum value of $S_s'(\kappa,\omega)$. For the data at 470 K, 526 K and 574 K we have 154, 282 and 370 data points, respectively. We determine the RMSD (listed in table 3) over the full κ range. In figure 10 we show $S_s'(\kappa,\omega)$ and the predictions from $S_s^{MC}(\kappa,\omega)$ and $S_s^{LO}(\kappa,\omega)$. We find that $S_s^{LO}(\kappa,\omega)$ gives a very good agreement with $S_s'(\kappa,\omega)$ at all three temperatures. The agreement between the other models for $S_s(\kappa,\omega)$ and $S_s'(\kappa,\omega)$ is significantly worse.

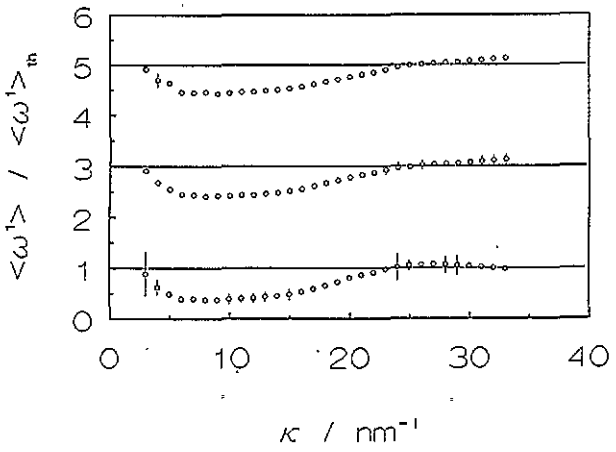

Figure 8. Ratio of $\langle\omega^1\rangle$ and the theoretical value for ^{7}Li at 470 K, 526 K (shifted by +2) and 574 K (shifted by +4).

Table 3. RMSD of the models for $S_s(\kappa,\omega)$ using no adjustable parameters with $S_s'(\kappa,\omega)$. The values used for ν, Ω and $\mathcal{D}$ (tracer data) are listed in table 2.

	$T = 470$ K	$T = 526$ K	$T = 574$ K
$S_s^{SD}(\kappa,\omega)$	1.79	1.44	1.79
$S_s^{MC}(\kappa,\omega)$	1.98	1.61	2.01
$S_s^{LO}(\kappa,\omega)$	1.36	0.93	1.11
$S_s^{NG}(\kappa,\omega)$	1.85	1.49	1.79

In figure 11 we show z_i/κ^2 of $S_s'(\kappa,\omega)$ and $\kappa^2 S_s'(\kappa,\omega=0)$ with the predictions from the four models for $S_s(\kappa,\omega)$.

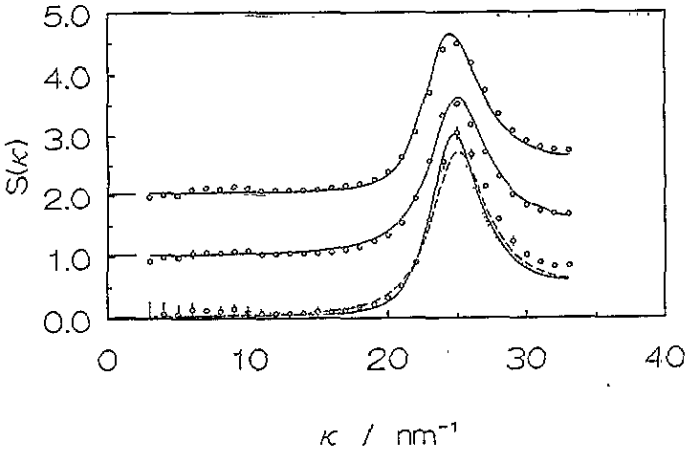

Figure 9. $S(\kappa)$ for ^{7}Li at 470 K, 526 K (shifted by +1.0) and 574 K (shifted by +2.0). Circles: present results. The diffraction data are listed in an overview article [26]. $S(\kappa)$ at 470 K (full curve: neutron diffraction data at 470 K [14]; broken curve: x-ray diffraction data at 464 K [13]; dotted curve: x-ray diffraction data at 463 K [22]), $S(\kappa)$ at 526 K (full curve: x-ray data at 523 K [22]), $S(\kappa)$ at 574 K (full curve: neutron diffraction data at 595 K [14],). The lines at $\kappa = 0$ denote $S(0)$.

We have also fitted the models for $S_s(\kappa, \omega)$ to $S'_s(\kappa, \omega)$ using one adjustable parameter. For $S_s^{SD}(\kappa, \omega)$ and $S_s^{MC}(\kappa, \omega)$ we fit $\mathcal{D}$, for $S_s^{NG}(\kappa, \omega)$ we fit α and for $S_s^{LO}(\kappa, \omega)$ we fit either $\mathcal{D}$ or Ω. For fitting Ω we use the tracer data for $\mathcal{D}$, for fitting $\mathcal{D}$ we use the theoretical values for Ω. The results are given in table 4. The uncertainty in the fitting parameter is determined using the F test with a 0.025 level of significance.

Table 4. Results of the fitting of models for $S_s(\kappa, \omega)$ with one adjustable parameter to $S'_s(\kappa, \omega)$. The entries in the table contain the value of the fitting parameter followed by the RMSD. $\mathcal{D}$ is given in units of 10^{-3} nm^{2}ps^{-1}, Ω and α are given in ps^{-1}.

	$T = 470$ K	$T = 526$ K	$T = 574$ K
$S_s^{SD}(\kappa, \omega)$ $\mathcal{D}$	5.9(2) : 1.62	8.2(1) : 1.02	10.1(1) : 1.10
$S_s^{MC}(\kappa, \omega)$ $\mathcal{D}$	6.5(3) : 1.99	9.1(3) : 1.61	11.4(2) : 1.99
$S_s^{LO}(\kappa, \omega)$ $\mathcal{D}$	6.7(2) : 1.35	9.1(1) : 0.92	11.1(1) : 1.17
$S_s^{LO}(\kappa, \omega)$ Ω	41(4) : 1.37	46(2) : 0.89	45(2) : 1.14
$S_s^{NG}(\kappa, \omega)$ α	94(4) : 1.71	75(1) : 1.28	65(1) : 1.60

In the hydrodynamic limit the ratio of the area of the Rayleigh mode to the area of the Brillouin modes is given by $(\gamma - 1)$, where $\gamma = c_p/c_V$ is close to unity for lithium (see table 2). Hence, in the hydrodynamic limit the Rayleigh mode comprises only a very small part of $S(\kappa)$. We observe a contribution centred around $\omega = 0$ in the present κ region. This has also been observed for lithium in INS experiments with PA analysis [10], in IXS experiments [3], and in CMD simulations of liquid lithium [6]. From the Lorentzian with half width z_0, representing the central contribution, we determine at 574 K an ionic thermal diffusion coefficient a_{ion} using $z_0 = a_{ion}\kappa^2$. The fitted value (0.13(3) nm^{2}ps^{-1}) is in good agreement with the result of CMD simulations of Gonzalez and co-workers [34] (0.14 nm^{2}ps^{-1}) using the neutral pseudo-atom (NPA) potential [5].

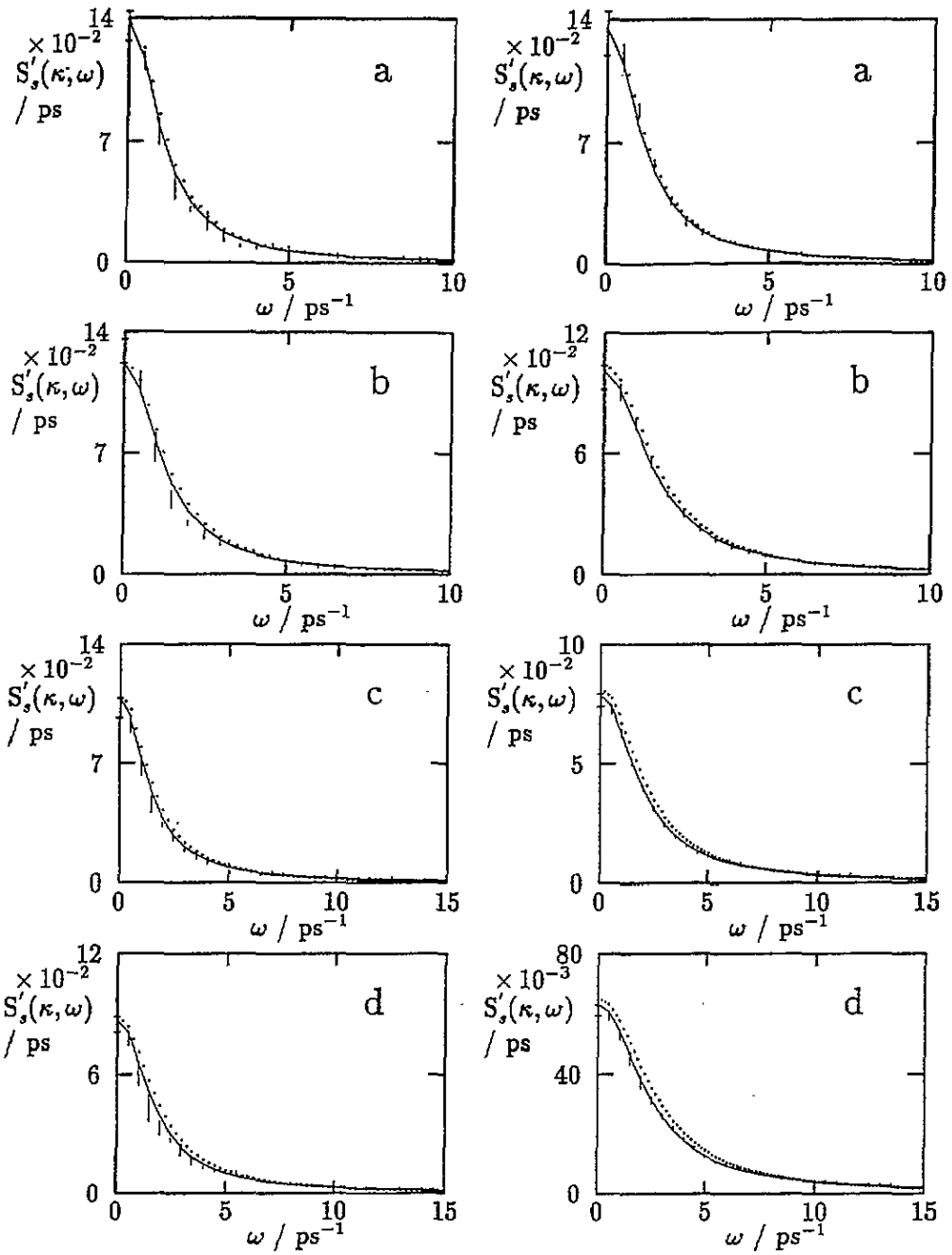

Figure 10. $S_s'(\kappa, \omega)$ for ^{7}Li at 470 K (left), 526 K (right) and 574 K (overleaf) at four selected κ-values. (*a*) $\kappa = 12\,\mathrm{nm}^{-1}$ ($14\,\mathrm{nm}^{-1}$ for ^{7}Li at 470 K), (*b*) $\kappa = 14\,\mathrm{nm}^{-1}$, ($15\,\mathrm{nm}^{-1}$ for ^{7}Li at 470 K), (*c*) $\kappa = 16\,\mathrm{nm}^{-1}$, (*d*) $\kappa = 18\,\mathrm{nm}^{-1}$. Error bars: experimental data; full line: $S_s^{\mathrm{LO}}(\kappa, \omega)$; dotted curve: $S_s^{\mathrm{MC}}(\kappa, \omega)$.

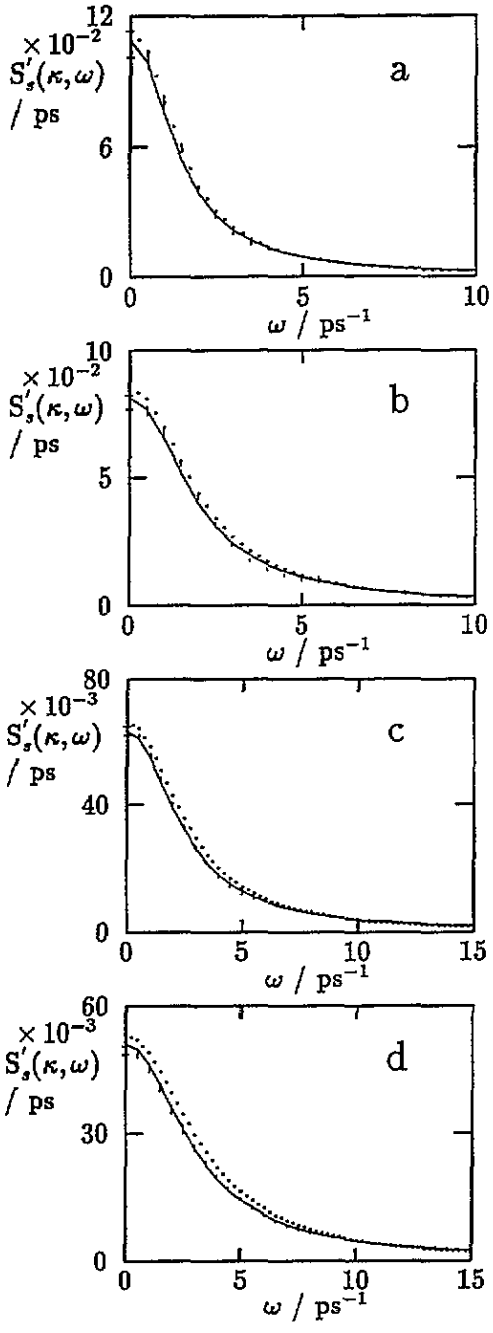

Figure 10. (Continued)

This is the first experimental value for a_{ion} since a_{ion} could not be determined from the INS experiment with PA analysis [10] or the IXS experiment [3]. The NPA potential is a suitable potential for liquid lithium because the results of the CMD simulation [6] are in good agreement with the present experimental data.

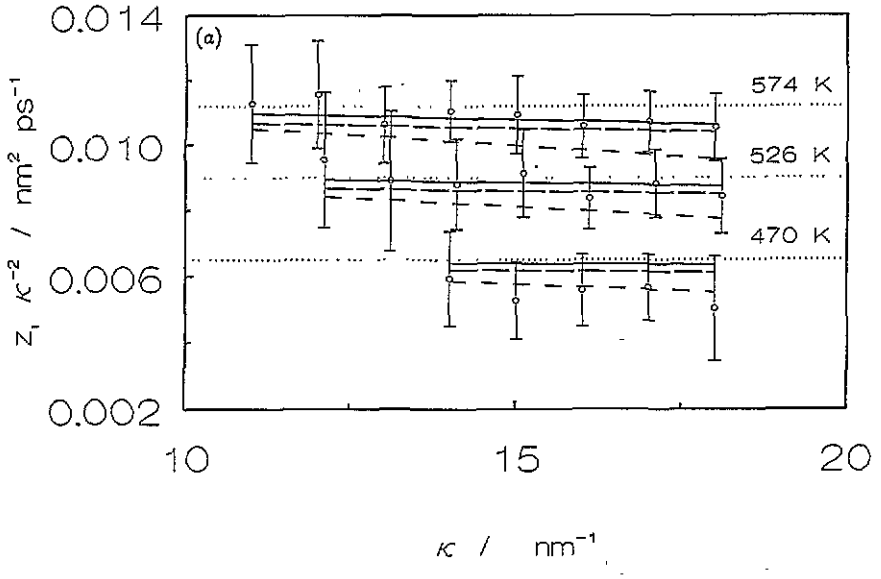

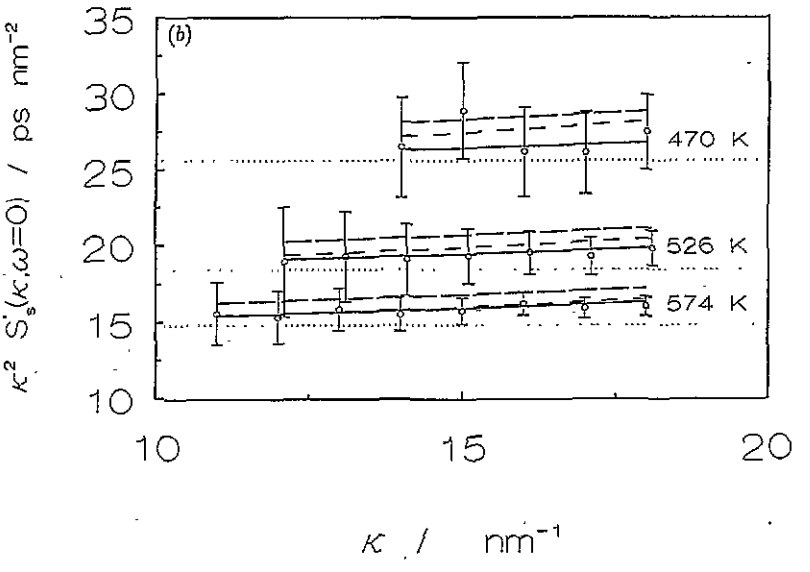

Figure 11. z_l/κ^2 (*a*) and $\kappa^2 S_s'(\kappa, \omega = 0)$ (*b*). Dotted line: predictions from $S_s^{SD}(\kappa, \omega)$; short-dash broken curve: predictions from $S_s^{LO}(\kappa, \omega)$; full curve: predictions from $S_s^{NG}(\kappa, \omega)$; long-dash broken curve: predictions from $S_s^{MC}(\kappa, \omega)$. The data at 526 K have been shifted by $+0.1\,\text{nm}^{-1}$ for clarity.

4.2.2. Dynamics near κ_0. In this section we discuss the separation of the coherent and the incoherent contributions near κ_0 using models for $S_s(\kappa, \omega)$ and $S_c(\kappa, \omega)$. We use the model of Nelkin–Ghatak $S_s^{NG}(\kappa, \omega)$ for $S_s(\kappa, \omega)$ [19] and we describe $S_c(\kappa, \omega)$ in terms of three extended hydrodynamic modes ($S_c^{EH}(\kappa, \omega)$). The number of free parameters, seven (α in $S_s^{NG}(\kappa, \omega)$, and the six parameters in $S_c^{EH}(\kappa, \omega)$), was reduced by imposing the first, first and second, and first through third frequency moments on $S_c^{EH}(\kappa, \omega)$. The weight factor w_{inc} (σ_i/σ_s) for $S_s^{NG}(\kappa, \omega)$ was determined from a fit to $S(\kappa, \omega)$ at small κ where $S_s(\kappa, \omega)$ dominates $S_c(\kappa, \omega)$. The fitted values 0.52(1) at 470 K, 0.51(1) at 526 K and 0.50(1) at 574 K are in reasonable agreement with the theoretical value (0.52(1)). The weight factor w_{coh} for $S_c^{EH}(\kappa, \omega)$ was taken as $(1 - w_{inc})$. Hence we have used

$$S(\kappa, \omega) = w_{inc} S_s^{NG}(\kappa, \omega) + w_{coh} S_c^{EH}(\kappa, \omega) \tag{4.2}$$

to fit the data. The RMSD of the weighted least-squares fit was of the order of unity. In figure 12 we show five parameters of the fits. The error bars connect the values obtained using different initial guesses for the fit parameters and from the fits with the first, first and second, and first through third frequency moments imposed.

5. Discussion

5.1. Static structure factor

We note the following about $S(\kappa)$ of liquid lithium.

(i) We have determined for the first time $S(\kappa)$ of liquid lithium by integration of $S_c(\kappa, \omega)$. The present $S(\kappa)$ are, apart from $S(\kappa)$ at 470 K beyond 26 nm^{-1}, in agreement with $S(\kappa)$ from literature. The largest deviations between the x-ray data and the neutron data from literature occur in the κ range 15–20 nm^{-1}. However, the accuracy of the present $S(\kappa)$ does not allow us to address the problem of differences between x-ray and neutron data.

(ii) The neutron diffraction experiment from Ruppersberg and Egger [14] at 470 K and at 595 K was made using neutrons with a small incident wavelength ($\lambda_0 = 0.0695$ nm). In a neutron diffraction experiment $S_c(\kappa, \omega)$ is integrated at each scattering angle by a detector along a curved path through κ–ω space. In figure 1 we show the integration path for a detector at a scattering angle of 2° using an incident wavelength of 0.0695 nm: this corresponds to the smallest scattering angle available in the experiment of Ruppersberg and Egger [14]. Recent experiments on liquid lithium [3, 9] provide indications that the position of the sound modes follow the expected behaviour (also given in figure 1) up to $\kappa_0/2$. Hence a considerable part of $S_c(\kappa, \omega)$ falls beyond the accessible ω range for small κ values in the neutron diffraction experiment [14]. The neutron diffraction data were normalized such that both the long- and short-wavelength limits were correct. Their $S(\kappa)$ might be influenced by this erroneous normalization procedure.

(iii) An accurate determination of $S(\kappa)$ of liquid lithium at small κ by neutron scattering is very difficult because of the low value of $S(0)$ (see table 2), the large incoherent contribution and the limited accessible ω range. Firstly, $\langle\omega^0\rangle$ has to be measured in an INS experiment with an accuracy better than 0.1% in order to have an accuracy of about 1% in $S(\kappa)$ (for $S(\kappa) \simeq 0.1$). Our present $\langle\omega^0\rangle$ has an accuracy of about 2% for a measuring time of about 90 h. Hence the duration of the present INS measurement will have to be prolonged by more than a factor 400. Secondly, the determination of $S(\kappa)$ is very sensitive to the values of the scattering cross sections of ^{7}Li. For example, if we use the listed values for the scattering cross sections ($\sigma_c = 0.619$ b and $\sigma_i = 0.68$ b, see table 1) and we

find $S(\kappa) = 0.05$ from the data analysis, then using values for the scattering cross sections ($\sigma_c = 0.625$ b and $\sigma_i = 0.65$ b) which lie within the uncertainty yields $S(\kappa) = 0.10$. This calculation shows that the determination of $S(\kappa)$ of liquid ^{7}Li requires more accurate values for the scattering cross sections. Finally, the determination of $S(\kappa)$ of liquid lithium at small κ by neutron diffraction measurements requires a large correction for inelastic effects. One either needs accurate experimental (or simulated) $S_c(\kappa, \omega)$ at small κ extending over a wide ω range or reliable models for $S_c(\kappa, \omega)$ in order to perform this correction properly.

5.2. Separation of the coherent and incoherent contributions

5.2.1. Dynamics at small κ. We note the following about our investigation of the dynamics at small κ.

(i) We have determined $S_s(\kappa, \omega)$ of a monatomic liquid at three temperatures close to the melting point. From a comparison of the experimental data with four models for $S_s(\kappa, \omega)$ using no adjustable parameters we find that $S_s^{LO}(\kappa, \omega)$ gives a very good description of $S_s'(\kappa, \omega)$ at all three temperatures. The agreement between $S_s'(\kappa, \omega)$ and the other models is significantly worse. The poor agreement between the experimental data and the models $S_s^{SD}(\kappa, \omega)$ and $S_s^{MC}(\kappa, \omega)$ in the present κ range is not remarkable considering that they are only valid in the hydrodynamic limit. We remark that $S_s(\kappa, \omega)$ of liquid Na close to the melting point [1] (using the values for $\mathcal{D}$ and Ω listed in table 1 of [1]) and liquid Ar [18] are also well described by the Lovesey model.

(ii) The reduced half width and reduced maximum value of $S_s'(\kappa, \omega)$ are not particularly useful quantities for comparing models with experimental data because they contain only a small part of the information available ($S_s'(\kappa, \omega)$). $S_s(\kappa, \omega)$ is a more sensitive quantity for testing models.

(iii) The best agreement between $S_s'(\kappa, \omega)$ and the models for $S_s(\kappa, \omega)$ with one adjustable parameter is obtained for $S_s^{LO}(\kappa, \omega)$ where we either fit $\mathcal{D}$ or Ω. The fitted $\mathcal{D}$ are in good agreement with the tracer data from Löwenberg and Lodding [29]. The fitted Ω value at 470 K is in good agreement with the theoretical result of Gonzalez and co-workers [32] and the fitted Ω at 526 K at 574 K are consistent with the predicted scaling relation from Levesque and Verlet [33]. The agreement between $S_s'(\kappa, \omega)$ and $S_s^{SD}(\kappa, \omega)$ improves considerably if we fit $\mathcal{D}$. However, the fitted $\mathcal{D}$ deviates considerably from the most accurate value in the literature. We cannot obtain good agreement between $S_s^{MC}(\kappa, \omega)$ and the experimental data by fitting $\mathcal{D}$. This shows that $S_s(\kappa, \omega)$ in the present κ range cannot be described by these hydrodynamic models. $S_s'(\kappa, \omega)$ can be reasonably well described by $S_s^{NG}(\kappa, \omega)$ by fitting α. The fitted value for α is slightly larger than its value in the hydrodynamic limit. The same occurs in liquid Na near the melting point [1]. We have assumed that α in liquid ^{7}Li near the melting point is κ independent, like α in liquid Na near the melting point. In order to investigate whether α is κ dependent we have fitted $S_s^{NG}(\kappa, \omega)$ to the data with a κ-dependent α. The RMSD, determined over the full κ range, improves by about 0.04. This shows that α is not strongly κ dependent.

(iv) $S_s^{MC}(\kappa, \omega)$, $S_s^{LO}(\kappa, \omega)$ and $S_s^{NG}(\kappa, \omega)$ predict that the reduced maximum value of $S_s(\kappa, \omega)$ approaches the hydrodynamic limit from above and that the reduced half width of $S_s(\kappa, \omega)$ approaches the hydrodynamic limit from below. One should therefore be cautious to conclude that mode-coupling might be relevant by merely studying these two quantities [7, 27].

(v) We can describe the temperature dependence of $\mathcal{D}$, determined from the fitting with $S_s^{LO}(\kappa, \omega)$, with an Arrhenius relation and with a model that has a linear temperature dependence. More accurate data for $\mathcal{D}$ extending over a wider temperature range are necessary to discriminate between theoretical models for $\mathcal{D}$ (e.g. [34]).

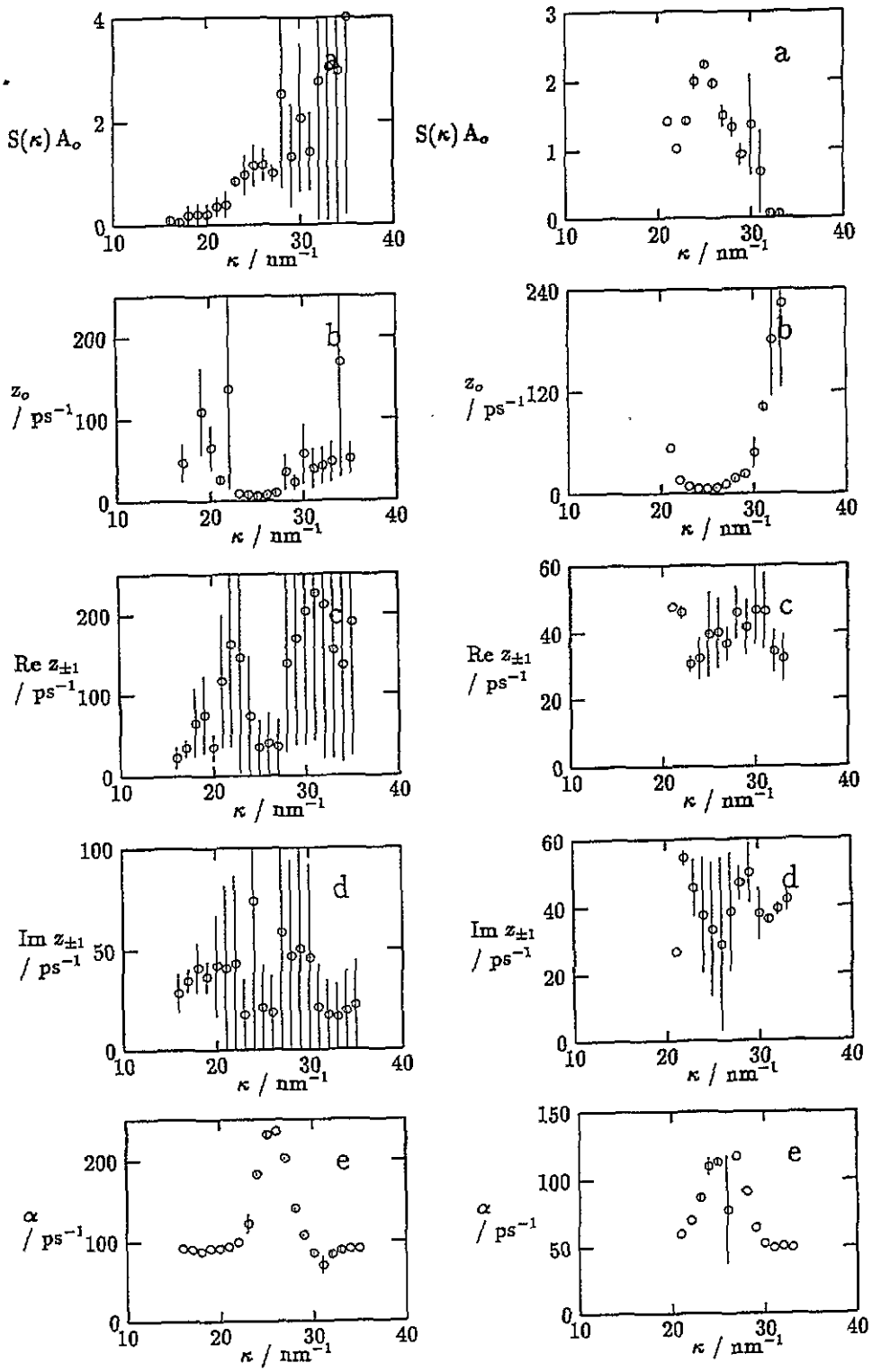

Figure 12. Parameters resulting from the fits of $S(\kappa, \omega)$ at 470 K (left), 526 K (right) and 574 K (facing page). (*a*) $S(\kappa)A_0$; (*b*) z_0; (*c*) $\mathrm{Re}z_{\pm 1}$; (*d*) $\mathrm{Im}z_{\pm 1}$ ($= \omega_s$); (*e*) α.

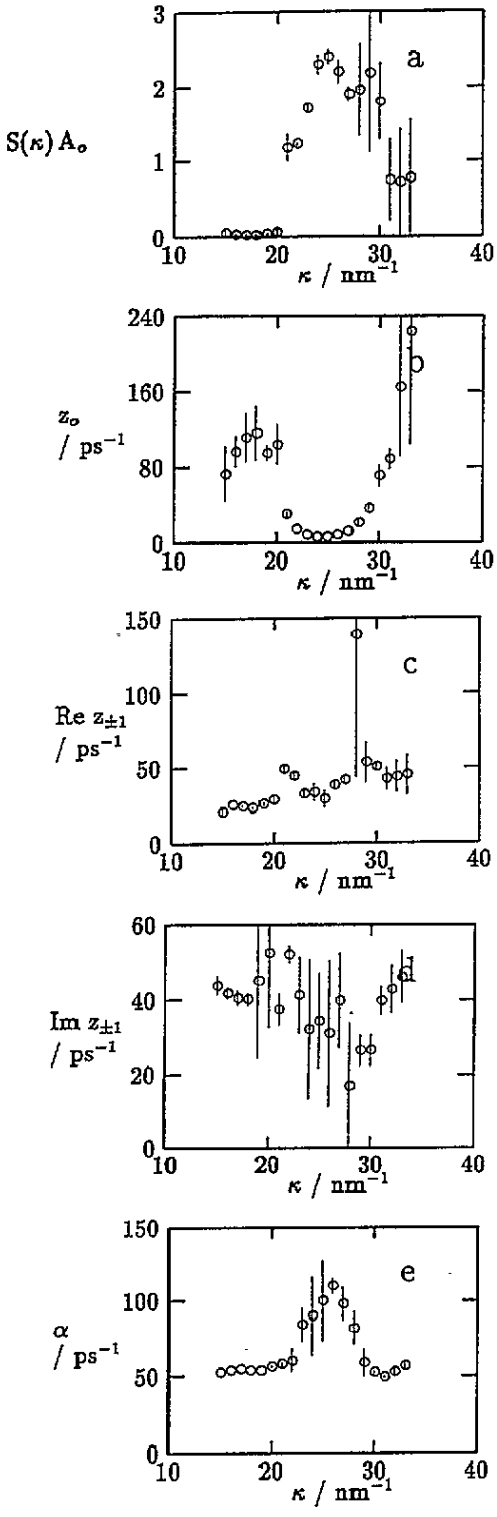

Figure 12. (Continued)

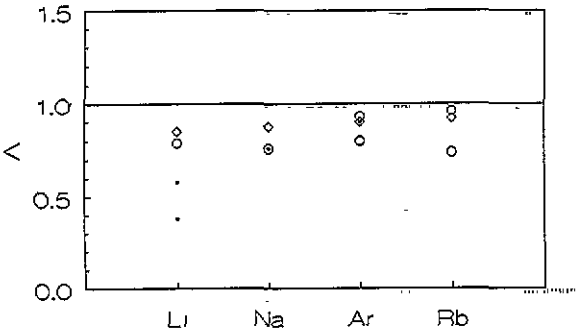

Figure 13. Λ for a number of liquids. The systems are arranged with increasing size of atoms. Dots: experimental results; lozenges: results of CMD simulations; circles: theoretical results. Li (circle: [10]; lozenge: [32]; dot (lower): present results at 470 K; dot (upper): present results at 526 K and 574 K); Na (lozenge: [49]; dot and circle: [1]); Ar (circle (upper): [50]; circle (lower): [51]; dot: [2]; lozenge: [33]); Rb (circle (upper); lozenge: [51]; circle (lower): [52]).

(vi) The differences between the models for $S_s(\kappa, \omega)$ in the present κ range are small. This is in contrast with the huge differences between the corresponding velocity autocorrelation functions $\Phi(t)$. For instance, in the hydrodynamic limit $\Phi(t)$ has an exponential decay whereas $\Phi(t)$ according to the Lovesey model has a prominent negative dip and shows oscillatory behaviour [18]. We remark that an experimental determination of the Fourier transform of $\Phi(t)$ by extrapolating $S_s(\kappa, \omega)$ to $\kappa \to 0$ is extremely difficult.

(vii) Morkel and co-workers [35] find indications for the existence of mode-coupling effects in liquid Na at 803 K. In order to study whether the same occurs in liquid lithium we performed additional measurements at higher temperatures (up to 843 K). The data analysis is under progress.

5.2.2. Dynamics near κ_0. From the fitting of models to the experimental data near κ_0 we find the following.

(i) The data at 470 K are inconclusive as to whether a sound propagation gap occurs (for example, as in liquid argon at moderate densities [36] or CMD simulations of Lennard-Jones liquids [37]) because the data can be described with a triplet (one extended Rayleigh mode and two extended Brillouin modes) as well as with a sum of three central Lorentzians. Overdamped sound modes in liquid lithium near the melting point are unlikely because collective modes are less damped in liquid metals. More accurate data with a good resolution are needed to give an unambiguous answer to this question. The data at 526 K and at 574 K provide indications that the collective modes extend beyond κ_0. This is very similar to the results on liquid Cs [38] near the melting point and to the results of experiments on liquid Ar [39] at a comparable density.

(ii) The widths of the sound modes near κ_0 appear to be proportional to κ; this has also been observed in experimental results (e.g. Cs [40]), in results from CMD simulations (i.e. Cs [41]) and in results of calculations (i.e. Zuilhof and co-workers [42]).

(iii) The value of α has a maximum near κ_0. The value of α is two times its value in the hydrodynamic limit (table 2). In liquid Na near the melting point [1] the increase of α with respect to its hydrodynamic value is only 25%. The maximum in α at κ_0 in liquid ^{7}Li results in a minimum in the reduced half width z_i/κ^2. In figure 13 we plot Λ ($= z_i(\kappa_0)/(\mathcal{D}\kappa_0^2)$) of a number of monatomic liquids for which $S_s(\kappa, \omega)$ is available; Λ, which is a measure of the deviation from simple diffusion, appears to be of the order of 10–20% for these systems. Our results suggest that the deviation from simple diffusion is much stronger in ^{7}Li than in other monatomic liquids.

(iv) We have inserted the half widths at κ_0 of the fitted $S_c^{\mathrm{EH}}(\kappa, \omega)$ at 526 K and 574 K in figure 2 of [43]. For σ we use the values determined in section 2. Our results show a clear deviation from the theoretical curve and the results for other dense fluids: the present data

are about 30% too high. A similar deviation occurs with the results from a CMD simulation of liquid lithium [28].

The anomalous behaviour of both $S_s(\kappa, \omega)$ and $S_c(\kappa, \omega)$ of liquid ^{7}Li with respect to other monatomic systems and theoretical models might be due to an incorrect separation of the coherent and incoherent contributions near κ_0. The most direct way to address this problem is by performing INS experiments with PA on liquid ^{7}Li. Efficient use of the neutrons is made when INS with PA is only used for the determination of $S_s(\kappa, \omega)$ and not for the determination of $S_c(\kappa, \omega)$; $S_c(\kappa, \omega)$ can then be determined by subtracting $S_s(\kappa, \omega)$ from the total $S(\kappa, \omega)$ measured without PA. Other ways to study this problem are to obtain more accurate INS data with an improved resolution near κ_0 or by making a detailed comparison with the results of CMD simulations of liquid lithium (see, for example, Canales and co-workers [6]).

6. Conclusions

We have reported on an INS experiment on liquid ^{7}Li at 470 K, 526 K and 574 K with the RKS spectrometer at our institute. The quality of the fully corrected $S(\kappa, \omega)$ is assessed by means of the detailed balance condition and by the first frequency moment $\langle\omega^1\rangle$ of $S(\kappa, \omega)$. We find that the data at all three temperatures satisfy the detailed balance condition; $\langle\omega^1\rangle$ can not be used as a consistency check for small κ because of the limited ω range. For $\kappa \geqslant 22\,\mathrm{nm}^{-1}$, $\langle\omega^1\rangle$ is in accord with the theoretical value.

$S(\kappa)$ of liquid ^{7}Li is determined by integration of $S_c(\kappa, \omega)$. The results are compared with $S(\kappa)$ from literature; $S(\kappa)$ at 470 K is in accord with x-ray data at 463 K and 464 K up to $23\,\mathrm{nm}^{-1}$ and with neutron data at 470 K up to $25\,\mathrm{nm}^{-1}$. For κ beyond $26\,\mathrm{nm}^{-1}$ the present $S(\kappa)$ at 470 K differs from the three other $S(\kappa)$; $S(\kappa)$ at 526 K is in agreement with x-ray data at 523 K and $S(\kappa)$ at 574 K is in agreement with neutron data at 595 K. The accuracy of the present $S(\kappa)$ does not allow for a comparison of the present neutron data with x-ray data. Hence more accurate data are needed for studying correlations between electrons and ions in liquid lithium.

We have determined the incoherent dynamic structure factor $S_s'(\kappa, \omega)$ from $S(\kappa, \omega)$ for κ up to $18\,\mathrm{nm}^{-1}$ by correcting for the coherent contribution. The data are compared with four models for $S_s(\kappa, \omega)$, namely the simple diffusion model, the mode-coupling model, the Lovesey model and the model of Nelkin–Gathak, using no adjustable parameters. We find that the Lovesey model gives the best agreement with the experimental data. The other models for $S_s(\kappa, \omega)$ give a poor description of the data. We remark that the Lovesey model also gives a good description of $S_s(\kappa, \omega)$ of liquid Ar and liquid Na near the melting point.

We have also fitted these four models for $S_s(\kappa, \omega)$ to $S_s'(\kappa, \omega)$ using one adjustable parameter. The Lovesey model gives the best agreement with the experimental data. The fitting parameter (either $\mathcal{D}$ or Ω) is in good agreement with independent results. The simple diffusion model with a fitted $\mathcal{D}$ gives a good agreement of the data. However, the value of $\mathcal{D}$ is too low with respect to the literature value. By fitting $\mathcal{D}$ we cannot obtain good agreement between the mode-coupling model and the experimental data. This means that the hydrodynamic models, simple diffusion and mode-coupling, cannot be used to describe the data in the present κ range. The agreement between the model of Nelkin–Ghatak with a κ-independent collision frequency α and the experimental data is reasonable. The value of α is slightly larger than its value in the hydrodynamic limit. This is similar to liquid Na near the melting point.

We have separated the coherent and incoherent contributions near κ_0, the position of the main peak of $S(\kappa)$, by fitting models. The reduced half width of $S_s(\kappa, \omega)$ shows a narrowing

near κ_0 which is much stronger than in other monatomic systems. On the other hand, the coherent contribution is broader than the results of a CMD simulation and broader than the predictions of a theoretical model which works very well for dense monatomic fluids. The anomalous behaviour of both the incoherent and coherent contribution might be due to an incorrect separation of the two contributions. This problem can be solved by performing INS experiments with polarization analysis on liquid ^{7}Li near κ_0 with good resolution.

Acknowledgments

The authors acknowledge financial support from the EC Science plan (SC1*CT91-0754).

References

[1] Morkel C and Gläser W 1986 *Phys. Rev.* A **33** 3383
[2] Sköld K, Rowe J M, Ostrowski G and Randolph P D 1972 *Phys. Rev.* A **6** 1107
[3] Burkel E 1991 *Inelastic Scattering of X-Rays with Very High Energy Resolution* (Berlin: Springer)
[4] Wentzcovitch R M and Martins J L 1991 *Solid State Commun.* **78** 831
[5] González L E, González D J, Silbert M and Alonso J A 1993 *J. Phys.: Condens. Matter* **5** 4283
[6] Canales M, Padro J A, González L E and Giro A 1993 *J. Phys.: Condens. Matter* **5** 3095
[7] de Jong P H K, Verkerk P, Ahda S and de Graaf L A 1992 *Recent Developments in the Physics of Fluids* ed W S Howells and A K Soper (Bristol: Institute of Physics Publishing) F233
[8] de Jong P H K, Verkerk P and de Graaf L A 1993 *J. Non-Cryst. Solids* **156–8** 48
[9] de Jong P H K, Verkerk P, de Graaf L A, Bennington S M, Howells W S, Taylor A D and Arai M 1994 unpublished
[10] Sedlmeir J 1992 *PhD thesis* Technical University Munich
[11] de Jong P H K 1993 *PhD thesis* Delft University of Technology
[12] Visser E G, Geertsma W, van der Lugt W and de Hosson J Th M 1980 *Z. Nat.* A **35** 373
[13] Olbrich H, Ruppersberg H and Steeb S 1983 *Z. Nat.* A **38** 1328
[14] Ruppersberg H and Egger H 1975 *J. Chem. Phys.* **63** 4095
[15] Chihara J 1989 *Phys. Rev.* A **40** 4507
[16] Takeda S, Inui M, Tamaki S, Maryuama M and Waseda Y 1993 *J. Non. Cryst. Solids* **156–8** 683
[17] de Schepper I M and Ernst M H 1979 *Physica* **98A** 189
[18] Lovesey S W 1973 *J. Phys. C: Solid State Phys.* **6** 1856
[19] Nelkin M and Ghatak A 1964 *Phys. Rev* **135** A4
[20] de Schepper I M and Cohen E G D 1980 *Phys. Rev.* A **22** 287
[21] de Schepper I M and Cohen E G D 1982 *J. Stat. Phys.* **27** 123
[22] Waseda Y 1980 *The Structure of Non-crystalline Materials, Liquids and Amorphous Solids* (New York: McGraw-Hill)
[23] Mayer H G 1994 Private communication
[24] Verkerk P and van Well A A 1985 *Nucl. Instrum. Meth.* **228** 438
[25] Aamodt R, Case K M, Rosenbaum M and Zweifel P F 1962 *Phys. Rev.* **126** 1165
[26] van der Lugt W and Alblas B P 1985 *Handbook of Thermodynamic and Transport Properties of Alkali Metals* ed R W Ohse (Oxford: Blackwell) p 299
[27] Montfrooy W, de Schepper I M, Bosse J, Gläser W and Morkel Ch 1986 *Phys. Rev.* A **33** 1405
[28] Canales M, González L E and Padro J A 1994 *Phys. Rev.* E at press
[29] Löwenberg L and Lodding A 1967 *Z. Nat.* A **22** 2077
[30] Murday J S and Cotts R M 1971 *Z. Nat.* A **26** 85
[31] Copley J R D and Lovesey S W 1975 *Rep. Prog. Phys* **38** 461
[32] González L E 1994 Private communications
[33] Levesque D and Verlet L 1970 *Phys. Rev.* A **2** 2514
[34] Murday J S and Cotts R M 1968 *J. Chem. Phys.* **48** 4938
[35] Morkel Ch, Gronemeyer Ch, Gläser W and Bosse J 1987 *Phys. Rev. Lett.* **58** 1873
[36] de Graaf L A *Static and Dynamic Properties of Liquids* ed M Davidović and A K Soper (Berlin: Springer) p 2

[37] de Schepper I M, van Rijs J C, van Well A A and de Graaf L A 1984 *Phys. Rev.* A **29** 1602
[38] Bodensteiner T, Morkel C, Gläser W and Dorner B 1992 *Phys. Rev.* A **45** 5709
[39] Verkerk P, van Well A A and de Schepper I M 1987 *J. Phys. C: Solid State Phys.* **20** L979
[40] Bodensteiner T 1990 *PhD thesis* Technical University Munich
[41] Kambayashi S and Kahl G 1992 *Phys. Rev.* A **46** 3255
[42] Zuilhof M J, Cohen E G D and de Schepper I M 1984 *Phys. Lett.* **103A** 120
[43] Cohen E G D, Westerhuijs P and de Schepper I M 1987 *Phys. Rev. Lett.* **59** 2872
[44] Sears V F 1986 *Methods of Experimental Physics* **23**: *Neutron Scattering A* ed K Sköld and D L Price (New York: Academic) p 533
[45] Dilg W 1974 *Nucl. Instrum. Methods* **122** 343
[46] Ohse R W (ed) 1985 *Handbook of Thermodynamic and Transport Properties of Alkali Metals* (Oxford: Blackwell)
[47] 1982 *Handbook of Chemistry and Physics* (Boca Raton, FL: CRC)
[48] Ban N T, Randall C M and Montgomery D J 1962 *Phys. Rev.* **128** 6
[49] Kinell T, Dahlborg U, Söderström O and Ebbsjö I 1985 *J. Phys. F: Met. Phys.* **15** 1033
[50] Wahnström G and Sjögren L 1982 *J. Phys. C: Solid State Phys.* **15** 401
[51] Götze W and Zippelius A 1976 *Phys. Rev.* A **14** 1842